Applications and Applied Mathematics: An International Journal (AAM)

Volume 12 | Issue 1 Article 12

6-2017

Analysis of Heat and Mass Transfer of an Inclined Magnetic Field Pressure-driven Flow Past a Permeable Plate

M. S. Dada
University of Ilorin

S. O. Salawu
University of Ilorin

Available at
http://pvamu.edu/aam
Appl. Appl. Math.
ISSN: 1932-9466

Applications and Applied Mathematics:
An International Journal
(AAM)

Vol. 12, Issue 1 (June 2017), pp. 189 - 200

Analysis of Heat and Mass Transfer of an Inclined Magnetic Field Pressure-driven Flow Past a Permeable Plate

M.S. Dada[1] and S.O. Salawu[2]

Department of mathematics
University of Ilorin
Ilorin, Nigeria
[1]dadamsa@gmail.com; [2]kunlesalawu@yahoo.com

Received April 5, 2016; Accepted April 3, 2017

Abstract

The study considers heat and mass transfer of magnetohydrodynamics pressure-driven flow passed a stretching permeable surface in the presence of inclined uniform magnetic field. The equations governing the model are transformed by Lie's group and solved using weighted residual method. The results obtained are compared with that of fourth order Runge-Kutta method that show the effects of Skin friction, Nusselt and Sherwood numbers on the flow. Finally, the influence of some important parameters on the flow are presented graphically and discussed.

Keywords: Lie group; Pressure-driven; Magnetic field; Permeable plate; Heat transfer; Mass transfer; Permeable surface

MSC 2010 No.: 76W05, 76D05

1. Introduction

Magnetohydrodynamic (MHD) deals with the combined effects of electromagnetic forces and fluid mechanics. It is the study of fluid that is electrically conducting such as liquid metals, plasmas, and electrolytes or salt water. The fundamental concept of MHD is that the magnetic field stimulates currents in a flowing conductive fluid and causes the magnetic field to change. A pressure-driven flow of heat and mass transfer in hydromagnetic fluid flow passed a permeable surface has being studied widely due to its importance in MHD power generators, reducing drag, MHD pumps, petroleum reservoirs, chemical catalytic reactor, Aeronautical engineering fields, nuclear waste disposal and others.

Youssef et al. (2007) reported on two-dimensional viscous fluid flow passed gradually contracting and expanding surfaces by means of frail porosity using Lie-group method. The authors neglected the pressure gradient and magnetic terms in their analysis while Mohammad et al. (2014) examined the flow of viscous fluid through contracting or expanding gaps in porous surfaces using optimal homotopy asymptotic method. In the study, the magnetic field term was neglected but considered the effect of Reynolds number on the pressure distribution. An analytical analysis was carried out on an inclined magnetic poiseuille flow through a parallel permeable sheets with a constant pressure gradient by Manyonge et al. (2012). It was found that the flow momentum reduced in the existence of suction/injection rates, inclined magnetic field, Hartmann number and pressure gradient. Also, the study of a non-Newtonian boundary layer of a power-law flow fluid in a convergent conduit was investigated by Pramanik (2013). In the analysis, the pressure gradient and magnetic field term was ignored while the equations governing the problem were transformed to nonlinear differential equations using scaling group of transformations. The cited authors above did not reflect on the influences of heat transfer as well as and mass transfer on the flow fluid.

The heat and mass transport under the effect of magnetic field has fascinated the attention of several intellectual scholars as a result of its applications in geophysics and astrophysics. Makinde (2010) gave analysis of heat exchange with the surrounding in a magnetodyrodynamic fluid flow with heat and mass transport over vertical boundary layer surface while Uwanta and Sarki (2012) studied heat and mass transfer by variable temperature along with exponential mass diffusion. The authors neglected the effect of pressure gradient in their study. Alireza (2013) reported on the magnetodyrodynamic stagnation point flow near a permeable stretching surface and chemical reaction. The problem was solved analytically using optimal homotopy asymptotic method and the results compared with fourth order Runge-Kutta method. Hossain and Samand (2013) investigated magnetodyrodynamic of heat and mass transfer flow with the existence of radiation, heat generation and chemical reaction through a stretching surface and magnetic field. The problem under consideration was transformed using similarity solution and solved numerically by applying shooting technique coupled with Runge-Kutta of fourth order scheme. Group transformation of dissipative hydromagnetic heat and mass transfer fluid flow over an inclined permeable plate was examined by Reddy (2013). The results show that the velocity increased as solutal and thermal Grashof numbers increased but decreased with a rise in Prandtl and Schmidt numbers. However, the pressure gradient, heat source and reaction rate terms did not reflect on the study.

Pressure-driven flow of heat and mass transfer in a magnetohydrodynamic are important in several engineering processes and it is then given a considerable attention by many researchers in recent years. In the processes like heat transfer in a cooling wet tower, fluid droplets sprays, purification of crud oil, flow in a desert cooler and possible applications in many industries which include water industry, petroleum industry, drilling industry, sewage treatment industry and many more are few areas where pressure-driven flow is applicable. MHD couette flow of time dependent pressure gradient in a casson fluid under the influence heat transfer was analyzed by Sayed-Ahmed et al. (2011). The flow was influenced by uniform magnetic field which was applied upright to the surface with regular and exponential pressure gradient, the flow was subjected to unvarying injection and suction. Farooq et al. (2013) examined steady poiseuille flow and heat transfer of couple stress fluids within two parallel inclined surfaces with variable viscosity. Reynold's model for temperature dependent viscosity was used. Thiagarajan and Sangeetha (2013) reported on nonlinear MHD flow with heat transfer through the boundary layer and pressure gradient in a vertical stretching surface in the existence of thermal conductivity and variable viscosity.

The above studies referred, neglected the influence of inclined magnetic field as well as the effects of

some fluid parameters on the fluid pressure. The current study examines the influence of inclined magnetic field on the flow and the effect of some fluid parameters on pressure drop in a steady heat and mass transfer of MHD flow.

2. Formulation of the Problem

Consider the convective heat and mass transfer of MHD pressure-driven flow of a steady, laminar, incompressible and viscous fluid flow through a permeable surface under the influence of uniform inclined magnetic field with pressure gradient. The motion of the fluid is maintained by both pressure gradient and gravity, and the flow is taken to be in the direction of x with y-axis normal to it. A uniform strength of magnetic field B_0 is applied at angle α lying in the range $0 < \alpha < \frac{\pi}{2}$ in the direction of the flow and $A = B = \frac{1}{l}$. The geometry and equations governing the two-dimensional MHD pressure-driven fluid flow passed a permeable surface with inclined magnetic field are as follows:

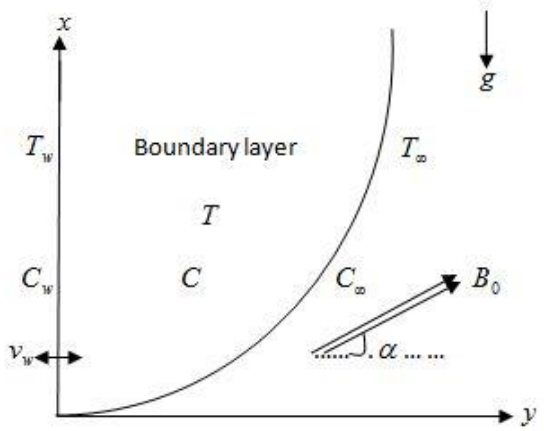

Figure 1: Geometry of the problem

$$\frac{\partial U}{\partial X} + \frac{\partial V}{\partial Y} = 0. \tag{1}$$

$$U\frac{\partial U}{\partial X} + V\frac{\partial U}{\partial Y} = -\frac{1}{\rho}\sigma B_0^2 U \sin^2\alpha - \frac{1}{\rho}\frac{\partial P}{\partial X} + \nu\left(\frac{\partial^2 U}{\partial X^2} + \frac{\partial^2 U}{\partial Y^2}\right) + g\beta_T(T - T_\infty) + g\beta_C(C - C_\infty). \tag{2}$$

$$U\frac{\partial V}{\partial X} + V\frac{\partial V}{\partial Y} = -\frac{1}{\rho}\frac{\partial P}{\partial Y} + \nu\left(\frac{\partial^2 V}{\partial X^2} + \frac{\partial^2 V}{\partial Y^2}\right). \tag{3}$$

$$\rho C_p\left(U\frac{\partial T}{\partial X} + V\frac{\partial T}{\partial Y}\right) = k\left(\frac{\partial^2 T}{\partial X^2} + \frac{\partial^2 T}{\partial Y^2}\right) + Q_0(T - T_\infty). \tag{4}$$

$$U\frac{\partial C}{\partial X}+V\frac{\partial C}{\partial Y}=D\left(\frac{\partial^2 C}{\partial X^2}+\frac{\partial^2 C}{\partial Y^2}\right)-\gamma\left(C-C_\infty\right). \tag{5}$$

The boundary and initial conditions are as follows.

$$\begin{aligned}&U=0,V=v_w,P=0,T=T_\infty+(T_w-T_\infty)AX,C=C_\infty+(C_w-C_\infty)BX\ \ at\ Y=0,\\&U=0,T=T_\infty,C=C_\infty\ \ as\ Y\to\infty.\end{aligned} \tag{6}$$

Using the following dimensionless quantities

$$x=\frac{X}{l},y=\frac{Y}{l},u=\frac{Ul}{\nu},v=\frac{Vl}{\nu},p=\frac{Pl^2}{\rho\nu^2},\theta=\frac{T-T_\infty}{T_w-T_\infty},\phi=\frac{C-C_\infty}{C_w-C\infty}. \tag{7}$$

Substituting dimensionless quantities (7) as well as the stream function

$$u=\frac{\partial\psi}{\partial y},\ \ v=-\frac{\partial\psi}{\partial x}$$

into Equations (1) to (6), we obtain

$$\frac{\partial\psi}{\partial y}\frac{\partial^2\psi}{\partial x\partial y}-\frac{\partial\psi}{\partial x}\frac{\partial^2\psi}{\partial y^2}=-H_a^2\sin^2\alpha\left(\frac{\partial\psi}{\partial y}\right)-\frac{\partial p}{\partial x}+\left(\frac{\partial^3\psi}{\partial x^2\partial y}+\frac{\partial^3\psi}{\partial y^3}\right)+G_r\theta+G_c\varphi, \tag{8}$$

$$-\frac{\partial\psi}{\partial y}\frac{\partial^2\psi}{\partial x^2}+\frac{\partial\psi}{\partial x}\frac{\partial^2\psi}{\partial x\partial y}=-\frac{\partial p}{\partial y}-\left(\frac{\partial^3\psi}{\partial x^3}+\frac{\partial^3\psi}{\partial x\partial y^2}\right), \tag{9}$$

$$\frac{\partial\psi}{\partial y}\frac{\partial\theta}{\partial x}-\frac{\partial\psi}{\partial x}\frac{\partial\theta}{\partial y}=\frac{1}{P_r}\left(\frac{\partial^2\theta}{\partial x^2}+\frac{\partial^2\theta}{\partial y^2}\right)+Q\theta, \tag{10}$$

$$\frac{\partial\psi}{\partial y}\frac{\partial\varphi}{\partial x}-\frac{\partial\psi}{\partial x}\frac{\partial\varphi}{\partial y}=\frac{1}{S_c}\left(\frac{\partial^2\varphi}{\partial x^2}+\frac{\partial^2\varphi}{\partial y^2}\right)-\lambda\varphi, \tag{11}$$

subject to the initial and boundary conditions

$$\begin{aligned}&\frac{\partial\psi}{\partial y}=0,\frac{\partial\psi}{\partial x}=f_w,p=0,\theta=x,\phi=x\ at\ y=0,\\&\frac{\partial\psi}{\partial y}=0,\theta=0,\phi=0\ as\ y\to\infty,\end{aligned} \tag{12}$$

where x and y are dimensionless coordinate, u and v are the dimensionless velocity, θ and ϕ are

the dimensionless temperature and concentration, p is the pressure, $H_a = lB_0\sqrt{\frac{\sigma}{\mu}}$ is the Hartmann number, $G_r = \frac{l^3 g\beta_T (T_w - T_\infty)}{\nu^2}$ is the thermal Grashof number, $GG_c = \frac{l^3 g\beta_C (C_w - C_\infty)}{\nu^2}$ is the solutal Grashof number, $P_r = \frac{\mu C_p}{k}$ is the Prandtl, $S_c = \frac{\nu}{D}$ is the Schmidt number, $Q = \frac{l^2 Q_0}{\mu C_p}$ is the heat source and $\lambda = \frac{l^2\gamma}{\nu}$ is the concentration parameter respectively. $f_w = -\frac{v_w l}{\nu}$ is the non-dimensional wall mass transfer coefficient such that $f_w \succ 0$ indicates wall suction and $f_w \prec 0$ indicates wall injection or blowing respectively.

Introducing Lie group of scaling transformations into Equations (8) - (12), (Mukhopadhyay et al. (2005) and Bhattacharyya et al. (2011)) as

$$\nabla : x^* = xe^{\varepsilon\alpha_1}, y^* = ye^{\varepsilon\alpha_2}, \psi^* = \psi e^{\varepsilon\alpha_3}, u^* = ue^{\varepsilon\alpha_4}, v^* = ve^{\varepsilon\alpha_5}, p^* = pe^{\varepsilon\alpha_6},$$
$$\theta^* = \theta e^{\varepsilon\alpha_7}, \phi^* = \phi e^{\varepsilon\alpha_8}, \tag{13}$$

where α_1, α_2, α_3, α_4, α_5, α_6, α_7 and α_8 are the parameters of transformation and ε is a small parameters. Equation (13) is regarded as a point-transformation that transforms coordinate $(x, y, \psi, u, v, \theta, \phi)$ to the coordinate $(x^*, y^*, \psi^*, u^*, v^*, \theta^*, \phi^*)$.

Using the transformations Equation (13) in Equations (8) - (12), these resulted to in one parameter group of transformations given by

$$x^* = xe^{\varepsilon\alpha_1}, y^* = y, \psi^* = \psi e^{\varepsilon\alpha_1}, u^* = ue^{\varepsilon\alpha_1}, v^* = v, p^* = p, \theta^* = \theta e^{\varepsilon\alpha_1}, \phi^* = \phi e^{\varepsilon\alpha_1}. \tag{14}$$

Then, the absolute invariant gives

$$f(\eta) = x^{*-1}\psi^*, p_d(\eta) = p^*, \theta(\eta) = x^{*-1}\theta^*, \phi(\eta) = x^{*-1}\phi^*. \tag{15}$$

Therefore, the similarity solutions become

$$\eta = y^*, \psi^* = x^* f(\eta), p^* = p_d(\eta), \theta^* = x^*\theta(\eta), \phi^* = x^*\phi(\eta). \tag{16}$$

Substituting the similarity solution of Equation (16) into Equations (8) to (12), to get the system of coupled differential equations;

$$f''' + ff'' - f'^2 - H_a^2 \sin^2\alpha f' + G_r\theta + G_c\phi = 0. \tag{17}$$

$$-p_d' = f'' + ff'. \tag{18}$$

$$\theta'' + P_r f\theta' - P_r f'\theta + P_r Q\theta = 0. \tag{19}$$

$$\phi'' + S_c f\phi' - S_c f'\phi - S_c \lambda\phi = 0. \tag{20}$$

The corresponding initial and boundary conditions transform to

$$\begin{aligned} &f = f_w,\ f' = 0,\ p_d = 0, \theta = 1, \phi = 1 \text{ as } \eta = 0, \\ &f' = 0, \theta = 0, \phi = 0 \text{ as } \eta \to \infty. \end{aligned} \tag{21}$$

Integrating Equation (18) with the initial and boundary conditions when $f_w = 1$, let pressure drop $-p_d = G$, this becomes

$$G = f' + \frac{1}{2} f^2 - \frac{1}{2}. \tag{22}$$

By applying WRM (McGrattan (1998) & Odejide and Aregbesola (2011)) to Equations (17) to (22), assuming a polynomial with unknown coefficients or parameters to be determined later, this polynomial is called the trial function which are defined as follow:

$$f(\eta) = \sum_{i=0}^{12} a_i \eta^i, \quad \theta(\eta) = \sum_{i=0}^{12} b_i \eta^i, \quad \phi(\eta) = \sum_{i=0}^{12} c_i \eta^i. \tag{23}$$

By imposing the boundary conditions (21) on the trial functions as well as substituting the trial functions into Equations (17), (19) and (20) to obtain the residual

$$\begin{aligned} f_r = {} & 6a_3 + 24a_4\eta + 60a_5\eta^2 + 120a_6\eta^3 + 210a_7\eta^4 + 336a_8\eta^5 + 504a_9\eta^6 + 720a_{10}\eta^7 \\ & + 990a_{11}\eta^8 + 1320a_{12}\eta^9 + P_r\left(f a_{12}\eta^{12} + f a_{11}\eta^{11} + f a_{10}\eta^{10} + f a_9\eta^9 + f a_8\eta^8 + \cdots\right) \end{aligned} \tag{24}$$

$$\begin{aligned} \theta_r = {} & 2b_2 + 6b_3\eta + 12b_4\eta^2 + 20b_5\eta^3 + 30b_6\eta^4 + 42b_7\eta^5 + 56b_8\eta^6 + 72b_9\eta^7 + 90b_{10}\eta^8 \\ & + 110b_{11}\eta^9 + 132b_{12}\eta^{10} + P_r\left(f a_{12}\eta^{12} + f a_{11}\eta^{11} + f a_{10}\eta^{10} + f a_9\eta^9 + f a_8\eta^8 + \cdots\right) \end{aligned} \tag{25}$$

$$\begin{aligned} \phi_r = {} & 2c_2 + 6c_3\eta + 12c_4\eta^2 + 20c_5\eta^3 + 30c_6\eta^4 + 42c_7\eta^5 + 56c_8\eta^6 + 72c_9\eta^7 + 90c_{10}\eta^8 \\ & + 110c_{11}\eta^9 + 132c_{12}\eta^{10} + S_c\left(a_{12}\eta^{12} + a_{11}\eta^{11} + a_{10}\eta^{10} + a_9\eta^9 + a_8\eta^8 + \cdots\right). \end{aligned} \tag{26}$$

The residual error are minimized to zero at some set of collocation points at a regular interval within the domain. That is,

$$\eta_k = \frac{(b-a)k}{N},$$

where $k = 1,2,...,N-1$ and $a = 0, b = 3, N = 11$. These are solved using MAPLE 18 to obtain the unknown coefficients.

Substituting the constant values into the trial functions to obtain the tangential velocity, temperature and concentration equations as follows;

$$f(\eta) = 1.000000000 - 2.099284624\eta^2 - 3.047632177\eta^3 + 2.530136715\eta^4 - 1.470259657\eta^5 + 0.6293250241\eta^6 - 0.1991658321\eta^7 + 0.0454804339\eta^8 - 0.0070852237\eta^9 + 0.00067064439\eta^{10} - 0.00002841484\eta^{11} - 0.000000010279\eta^{12}. \quad (27)$$

$$\theta(\eta) = 1.000000000 - 0.7501015305\eta - 0.08820358330\eta^2 + 0.6074318152\eta^3 - 0.7261180797\eta^4 + 0.5709303379\eta^5 - 0.3295917512\eta^6 + 0.1429428400\eta^7 - 0.04630653096\eta^8 + 0.01089292777\eta^9 - 0.001757153433\eta^{10} + 0.0001735751976\eta^{11} - 0.000007901449859\eta^{12}. \quad (28)$$

$$\phi(\eta) = 1.000000000 - 1.420604887\eta + 0.7550189757\eta^2 + 0.1114517669\eta^3 - 0.5521183085\eta^4 + 0.5564172609\eta^5 - 0.3637757365\eta^6 + 0.1733374400\eta^7 - 0.06091843489\eta^8 + 0.01538962724\eta^9 - 0.002639573886\eta^{10} + 0.0002746098028\eta^{11} - 0.00001305341620\eta^{12}. \quad (29)$$

Differentiate Equation (27) to obtain

$$f'(\eta) = 4.198568249\eta - 9.142898325\eta^2 + 10.12054343\eta^3 - 7.351298528\eta^4 + 3.775950145\eta^5 - 1.394160825\eta^6 + 0.3638434712\eta^7 - 0.0637670133\eta^8 + 0.00670644390\eta^9 - 0.00031256324\eta^{10} - 0.00000123348\eta^{11}. \quad (30)$$

Substituting for f and f' in Equation (22) with the constant values to obtain the pressure drop as,

$$G(\eta) = -0.5000000000 + 4.198568249\eta - 9.142898325\eta^2 + 10.12054343\eta^3 - 7.351298285\eta^4 + 3.775950145\eta^5 - 1.394160825\eta^6 + 0.3638434716\eta^7 - 0.06376701332\eta^8 + 0.006706443900\eta^9 - 0.0003125631885\eta^{10} - 0.000001233432062\eta^{11} + 1/2\left(1.000000000 + 2.099284246\eta^2 - 3.047632127\eta^3 + 2.530136764\eta^4 - 1.470257995\eta^5 + 0.6293250241\eta^6 - 0.1991658321\eta^7 + 0.04548043395\eta^8 - 0.007085223702\eta^9 + 0.0006706443900\eta^{10} - 0.00002841483532\eta^{11} - 0.0000001027860052\eta^{12}\right)^2. \quad (31)$$

Skin Friction

$$\tau = \frac{\partial^2 f}{\partial \eta^2} = 4.198568249 - 18.28579665\eta + 30.36163283\eta^2 - 29.40519431\eta^3 + 18.87975072\eta^4 - 8.364964948\eta^5 + 2.546904301\eta^6 - 0.5101361065\eta^7 + 0.06035799510\eta^8 - 0.003125631885\eta^9 - 0.00001356775269\eta^{10}. \quad (32)$$

Nusselt Number

$$\begin{aligned} Nu = -\frac{\partial \theta}{\partial \eta} = {} & 0.7501015305 + 0.1764071666\eta - 1.822295464\eta^2 + 2.904472293\eta^3 \\ & - 2.854651690\eta^4 + 1.977550507\eta^5 - 1.000599880\eta^6 + 0.3704522477\eta^7 \\ & - 0.09803634993\eta^8 + 0.01757153433\eta^9 - 0.001909327174\eta^{10} \\ & + 0.00009481739831\eta^{11}. \end{aligned} \tag{33}$$

Sherwood Number

$$\begin{aligned} Sh = -\frac{\partial \phi}{\partial \eta} = {} & 1.420604887 - 1.510037951\eta - 0.3343553007\eta^2 + 2.208473423\eta^3 - 2.782086240\eta^4 \\ & + 2.182654419\eta^5 - 1.213362080\eta^6 + 0.4873474791\eta^7 - 0.1385066452\eta^8 \\ & + 0.02639573886\eta^9 - 0.003020707831\eta^{10} + 0.0001566409944\eta^{11}. \end{aligned} \tag{34}$$

The process of weighted residual method are repeated for different values of G_r, G_c, H_a, α, Q, P_r, S_c and λ.

The following computational results in the table were obtained and compared well with shooting technique coupled with fourth order Runge-kutta method.

Table 1: Comparison of τ, Nu and Sh for various values of G_r, G_c, Q and S_c (PP-Physical Parameters)

		Weighted Residual method			4^{th} order R-K		
PP	values	τ	*Nu*	*Sh*	τ	*Nu*	*Sh*
G_r	2.5	2.86521	0.53944	1.34943	2.86359	0.53931	1.34902
	5.5	3.77012	0.69197	1.39921	3.76616	0.69173	1.39866
	7	4.19857	0.75010	1.42060	4.19315	0.74981	1.41999
G_c	4.5	3.59067	0.68694	1.39516	3.58741	0.68673	1.39467
	5.5	3.83489	0.71293	1.40549	3.83083	0.71269	1.40495
	7	4.19857	0.75010	1.42060	4.19315	0.74981	1.41998
Q	0.3	4.02001	1.08149	1.40258	4.01476	1.08098	1.40195
	1.0	4.19857	0.75010	1.42060	4.19315	0.74981	1.41998
	2.0	4.63757	0.01876	1.46429	4.63208	0.01877	1.46368
S_c	0.01	4.79802	0.93631	0.35822	4.79293	0.93598	0.35822
	0.1	4.65693	0.89254	0.56181	4.65179	0.89221	0.56179
	0.62	4.19857	0.75010	1.42061	4.193156	0.74981	1.41999

3. Results and Discussion

The computational analysis has been investigated by applying weighted residual method to the resultant equations for variations in the governing parameters, the Hartmann number H_a, angle of inclination α, thermal Grashof number G_r, heat source Q, Schmidt number S_c, Prandtl number P_r, solutal Grashof number G_c, and reaction rate parameter λ. The subsequent values are set as the default parameters for the computation: $G_r = G_c = 7$, $Q = \lambda = 1$, $P_r = 0.72$, $S_c = 0.62$, $H_a = 5$ and $\alpha = 30^0$. The graphs trail these values unless otherwise stated.

Table 1 shows the effect of some parameters on skin friction, sherwood and nusselt numbers. It is clearly seen that a rise in the solutant and thermal Grashof numbers have an accelerating effect on the skin friction, sherwood and nusselt numbers. An increase in heat source parameter enhances the sherwood number and skin friction while it retards the Nusselt number because heat within the boundary layer reduces. Also, nusselt number and skin friction reduces as the schmidt number rises but have an increasing effect on the sherwood number.

Figures 2 and 3 illustrate the velocity and pressure distributions for diverse values of Hartmann number H_a. It is observed that as the values of magnetic field parameter H_a is rising, the velocity and pressure profiles decreases because of the Lorentz force from the magnetic field which retarded convective fluid flow.

Figures 4 and 5 show the pressure and velocity distributions for different angles of inclination of the magnetic field α, while other parameters are kept fixed at some values. A rise in the degree of inclination α resulted in an increase in the effect of the buoyancy force and thereby reduces the force driven the fluid flow. Consequently, the momentum and pressure boundary layers decreases.

Figures 6 and 7 represent the influence of the heat source Q on the pressure and temperature profiles. It is noticed that the pressure and temperature distributions rise speedily due to a rise in the parameter value Q. The figures specify that a rise in the parameter Q, speed up the pressure and thermal boundary layers thickness which in turn enhances the pressure and slows down the energy transfer coefficient at the plate.

Figures 8 and 9 represent the effects of chemical reaction rate parameter λ on the pressure and concentration distributions. An increase in the values of λ, decreases the pressure profiles as seen in Figure 8. From Figure 9, it is very clear that the reactive solutal profile decrease with a rise in the values of λ. That is, the reaction rate parameter is a decreasing agent and as a result, the solute boundary layer close to the wall becomes thinner. This is as a result of the change of species which is experienced near the wall due to the presence of chemical reaction and then decreases the concentration in the boundary layer.

4. Conclusion

The governing equations of the flow model under consideration are non-dimensionalised and transformed to a coupled ordinary differential equations using Lie group. From the results, it was found that, a rise in the values of the magnetic field parameter Hartmann or degree of inclination of the magnetic field is manifested as a decrease in the flow velocity and pressure profiles. The pressure and temperature distributions is seen to increase gradually as the heat source increases while an increase in the chemical reaction rate reduces the pressure and concentration distributions. The results of this research has wide

areas of applications in pure sciences which includes oceanography, atmospheric sciences, geophysics etc. and in technology such as waste disposal, pollution dispersal, aerospace propulsion systems, manufacturing processes and many more.

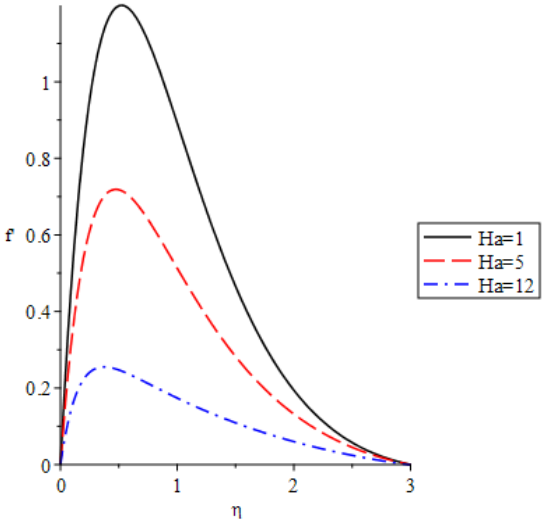

Figure 2: Velocity profiles for different values of Ha

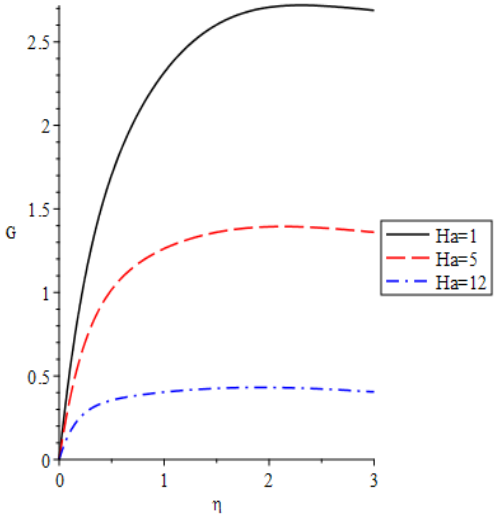

Figure. 3: Pressure profiles for different values of Ha

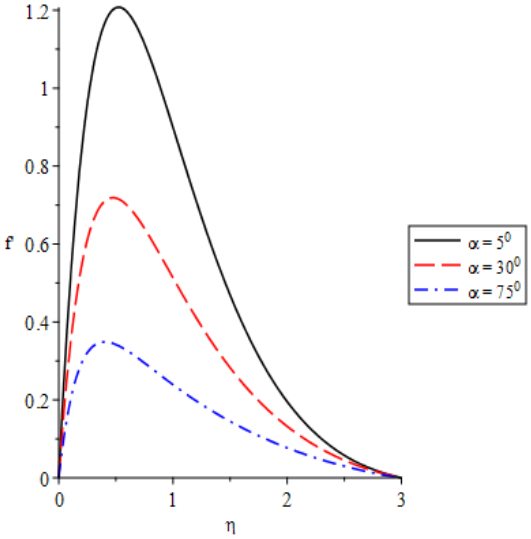

Figure 4: Velocity profiles for different values of α

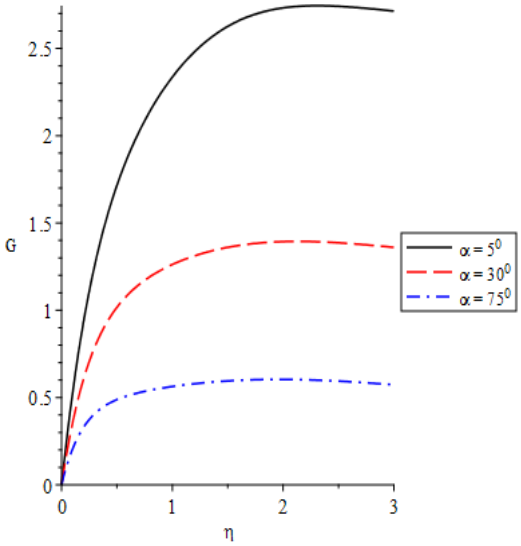

Figure 5: Pressure profiles for different values of α

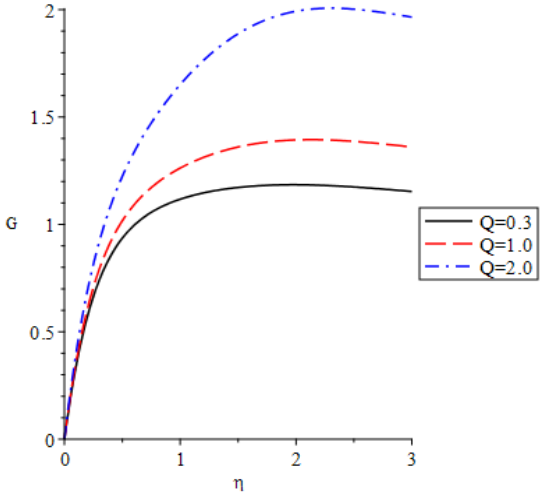

Figure 6: Pressure profiles for different values of Q

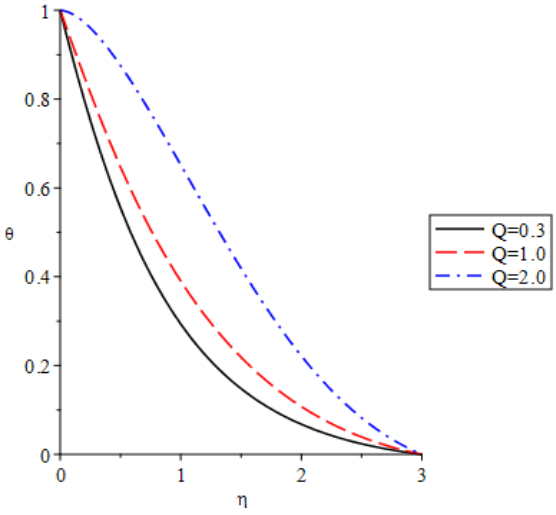

Figure 7: Temperature profiles for different values of Q

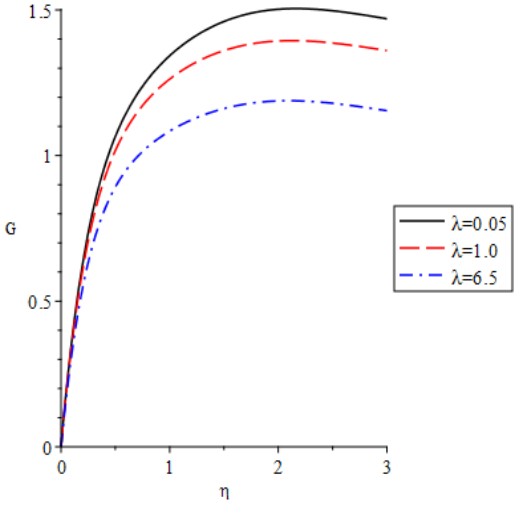

Figure 8: Pressure profiles for different values of λ

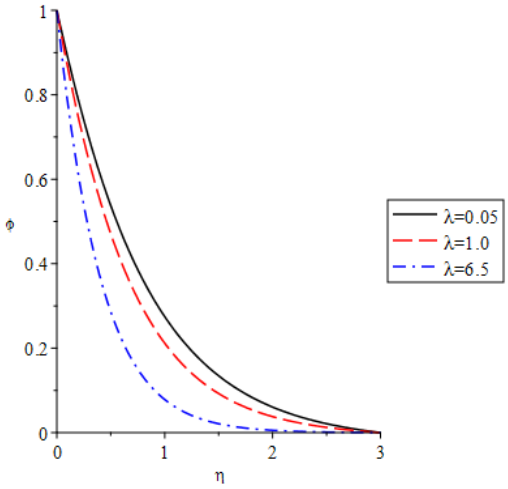

Figure 9: Concentration profiles for different values of λ

REFERENCES

Alireza, R., Mahmood, F. and Seyed, R.V. (2013). Analytical solution for magnetohydrodynamic stagnation point flow and heat transfer over a permeable stretching sheet with chemical reaction. Journal of Theoretical and Applied Mechanics, 51(3), 675-686.

Bhattacharyya, K., Uddin, M.S. and Layek, G.C. (2011). Application of scaling group of transformations to steady boundary layer flow of newtonian fluid over a stretching sheet in presence of chemical reactive species. Journal of Bangladesh Academy of Sciences, 35(1), 43-50.

Farooq, M., Rahim, M.T., Islam, S. and Siddiqui, A.M. (2013). Steady poiseuille flow and heat transfer couple stress fluids between two parallel inclined plates with variable viscosity, Journal of the Association of Arab Universities for Basic and Applied science, 14, 9-18.

Hossain, M.S. and Samand, M.A. (2013). Heat and mass transfer of an MHD free convection flow along a stretching sheet with chemical reaction, radiation and heat generation in presence of magnetic field. Research Journal of Mathematics and Statistics, 5(1-2), 05-17.

Makinde, O.D. (2010). On MHD heat and mass transfer over a moving vertical plate with a convective surface boundary condition. The Canadian Journal of Chemical Engineering, 9999, 700-710.

Manyonge, W.A., Kiema, D.W. and Iyaya, C.C. (2012). Steady MHD poiseuille flow between two infinite parallel porous plates in an inclined magnetic field. International Journal of Pure and Applied Mathematics, 76(5), 661-668.

McGrattan E.R. (1998). Application of weighted residual mehtods to dynamic economics models. Federal Reserve Bank of Minneapolis Research Department Staff Report, 232.

Mohammad, M.R., Esmaeel, E. and Behnam, R. (2014). Optimal homotopy asymptotic method for solving viscous flow through expanding or contracting gaps with permeable walls, Transaction on IoT and Cloud Computing, 2(1), 76-100.

Mukhopadhyay, S., Layek, G.C. and Samad, S.A. (2005). Study of MHD boundary layer flow over a heated stretching sheet with variable viscosity. Int. J. Heat Mass Transfer, 48, 60-66.

Odejide, S.A. and Aregbesola, Y.A.S. (2011). Applications of method of weighted residuals to problems with semi-finite domain. Rom. Journ. Phys., 56(1-2), 14-24.

Pramanik, S. (2013). Applications of scaling group of transformations to the boundary layer flow of a non-newtonian power-law fluid. Int. journal of Appl. Math and Mech., 9(6), 1-13.

Reddy, M.G. (2013). Scaling transformation for heat and mass transfer effects on steady MHD free convection dissipative flow past an inclined porous surface. Int. journal of Appl. Math. and Mech., 9(10), 1-18.

Sayed-Ahmed, M.E., Hazem A.A. and Karem M.E. (2011). Time dependent pressure gradient effect on unsteady MHD couette flow and heat transfer of a casson fluid. Scientific Research, 3(11), 38-49.

Thiagarajan, M. and Sangeetha, A.S. (2013). Nonlinear MHD boundary layer flow and heat transfer past a stretching plate with free stream pressure gradient in presence of variable viscosity and thermal conductivity. United States of America Research Journal, 1(4), 25-31.

Uwanta, I.J. and Sarki, M.N. (2012). Heat and mass transfer with variable temperature and exponential mass diffusion. International Journal Of Computational Engineering Research, 2(5), 1487-1494.

Youssef, Z.B., Mina, B.A., Nagwa, A.B. and Hossam, S.H. (2007). Lie-group method solution for two-dimensional viscous flow between slowly expanding or contracting walls with weak permeability. Applied Mathematical Modelling, 31(2007), 1092-1108.